2010-11

Growth kinetics of vanadium pentoxide nanostructures under hydrothermal conditions

Journal of Crystal Growth, Amsterdam : Elsevier,v. 312, n.23, p. 3555-3559, Nov 2010
http://www.producao.usp.br/handle/BDPI/50041

Journal of Crystal Growth 312 (2010) 3555–3559

Contents lists available at ScienceDirect

Journal of Crystal Growth

journal homepage: www.elsevier.com/locate/jcrysgro

Growth kinetics of vanadium pentoxide nanostructures under hydrothermal conditions

Waldir Avansi Jr.[a,*], Cauê Ribeiro[b], Edson R. Leite[c], Valmor R. Mastelaro[a]

[a] Instituto de Física de São Carlos, Universidade de S. Paulo, São Carlos, SP, Brasil
[b] Embrapa, Empresa Brasileira de Pesquisas Agropecuárias, São Carlos, SP, Brasil
[c] LIEC—DQ/UFSCAR, Universidade Federal de São Carlos, São Carlos, SP, Brasil

ARTICLE INFO

Article history:
Received 20 June 2010
Accepted 3 September 2010
Communicated by J.M. Redwing
Available online 22 September 2010

Keywords:
A1. Crystal growth
A1. Oriented attachment
A2. Hydrothermal treatment
B1. Vanadium pentoxide

ABSTRACT

The work reported here involved a study of the growth kinetics of $V_2O_5nH_2O$ nanostructures under hydrothermal conditions. The coarsening process of $V_2O_5nH_2O$ nanoribbons was followed by subjecting the as-prepared suspensions to hydrothermal treatments at 80 °C for periods ranging from 0 to 7200 min. X-ray diffraction (XRD) confirms that the hydrothermal treatments at 80 °C caused no significant modification of the long-range order structure of samples subjected to different periods of hydrothermal treatment. Field emission scanning transmission electron microscope (FE-STEM) was used to analyze the morphology and width distribution of the nanostructures. The results indicated that the crystal growth mechanism in the [1 0 0] direction of vanadium pentoxide 1D nanostructure under hydrothermal conditions is well described by the oriented attachment (OA) mechanism. This evidence was supported by HRTEM images showing the existence of defects at the interface between nanostructures, which is characteristic of the oriented attachment (OA) mechanism.

1. Introduction

Vanadium oxide 1D nanostructures have attracted the interest of many researches in the last decade due to their chemical and physical properties and their great potential for application in catalysis [1], photocatalytic activities [2], as sensors [3–6] and in electrochromic devices [7].

The literature contains several reports about the synthesis of vanadium oxide 1D nanostructures [2,3,8–11]. The hydrothermal method has been used extensively to obtain high anisotropic nanostructures, since it allows for the modification of synthesis parameters such as reaction temperature, pH and solvent concentration, as well as the addition of templates or additives, making it possible to obtain samples with different morphologies and structures [2,3,12–15]. The possibility of varying these synthesis parameters is important since technological applications of nanostructured materials are strongly related to their crystalline structure, crystal size and morphology.

In this approach, knowledge of the crystal growth mechanism of nanomaterials is very important in order to obtain controlled nanostructures. The Ostwald ripening (OR) model, which is a dissolution-reprecipitation growth mechanism, is a common process of the crystal growth mechanism assigned to several nanomaterials [16]. On the other hand, a different mechanism, known as oriented attachment (OA) or "cementing mechanism", has also proved to be an effective mechanism to describe the anisotropic growth of some nanomaterials [17–23]. It has been proposed that the OA mechanism may occur in two ways for colloids: (1) nonaligned particles undergo crystallographic rotations until a favorable geometry is obtained and coalescence takes place, and (2) coalescence may occur by effective collision between particles with the same crystallographic orientation. The former is possible when particle-to-particle contact occurs, as in agglomerates for example, while the latter is the dominant mechanism in dispersed suspensions [17–21]. After collisions in a particular crystallographic orientation, the coalescence of nanoparticles leads to the formation of defects such as dislocations and/or twin boundaries at the interface between nanoparticles [18,20]. Some parameters such as the treatment temperature and concentration of suspensions, which are related to the collision frequency between nanoparticles, are important to increase coalescence in the OA mechanism [20]. In addition, it seems that the anisotropic growth may be controlled through the introduction of different additives during the reaction [24].

Recently, Ribeiro et al. [25] applied a "polymeric" approach, which interprets particle coarsening analogously to polycondensation reactions to describe the structural formation of anisotropic nanoparticles in colloidal suspensions. In this model, called the polymerization-oriented attachment model (polymerization OA model), formation of the structure may be interpreted as the

* Corresponding author. Tel.: +55 16 3373-9828.
E-mail address: w_avansi@if.sc.usp.br (W. Avansi Jr.).

0022-0248/$ - see front matter © 2010 Elsevier B.V. All rights reserved.
doi:10.1016/j.jcrysgro.2010.09.010

connection of two active surfaces, like in a polymerization reaction. The equation that describes the crystal growth kinetics in the polymerization OA model is given by

$$x_{max} = -\frac{1}{\alpha \ln(8\sqrt{2k_0[S]_0 t}/1 + 8\sqrt{2k_0[S]_0 t})} \quad (1)$$

where x_{max} indicates the degree of coalescence related to the size of nanostructures as a function of treatment time and the size of primary particles, i.e., particles that do not coalesce. The term S_0 represents the initial concentration of active surfaces, t is the time of treatment and α a constant related to the particles, which are considered as monomers and are involved in the coarsening process. An important feature of this model is the applicability in any direction of the crystal growth, i.e., an independent analysis can be made in each direction in the final particle morphology, since the primary assumptions of the model are dependent only on the number of connected particles [25].

Based on these trends, the aim of this work is to verify which growth mechanism is present during the formation of vanadium pentoxide 1D nanostructures. To the best of our knowledge, this is the first time such an evaluation using the OA mechanism has been done in the case of $V_2O_5nH_2O$ nanostructures obtained under hydrothermal conditions. No surfactant, ligants or monomers were added to the solution in order to minimize the effects that could affect the crystal growth kinetics.

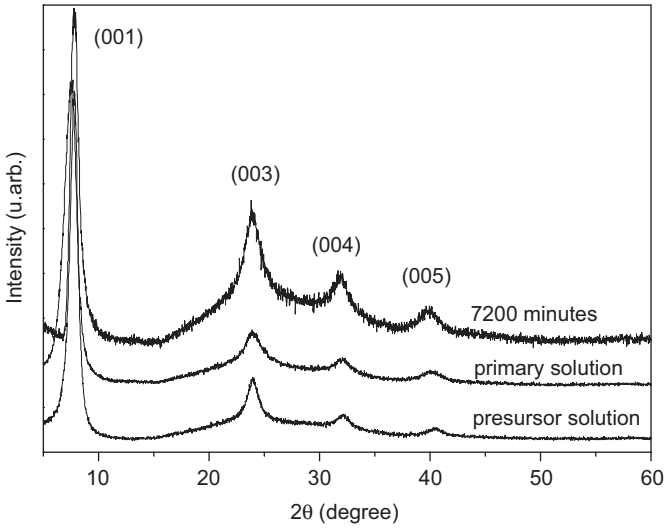

Fig. 1. XRD patterns of samples obtained from the precursor solution, the primary solution (0 min of heat-treatment) and the solution subjected to 7200 min of treatment.

2. Experimental section

The synthesis of $V_2O_5nH_2O$ nanostructures obtained in hydrothermal conditions, which is described in greater detail elsewhere by Avansi et al. [26], is based on the dissolution of 0.06 M of V_2O_5 powder in distilled water with the addition of 30% H_2O_2 and then subjected in hydrothermal treatment. The samples used to study the growth kinetics of $V_2O_5nH_2O$ nanostructures were obtained by hydrothermal treatment at 80 °C for 4 h. After synthesis, the solution was subjected to a treatment in ultrasound for 30 min to ensure the total decomposition of the peroxide. According to our previous work, this solution consists of a stable colloidal suspension of $V_2O_5nH_2O$ presenting a nanoribbon morphology [26]. For the sake of clarity, this solution is referred to as precursor solution. To follow the kinetics of crystal growth, this sample was diluted in distilled water to obtain a solution with 0.006 M of $V_2O_5nH_2O$. This "new solution" was subjected for a second time to hydrothermal treatment at 80 °C for periods of time ranging from "0" to 7200 min. The solution prepared at 80 °C with "0" min of treatment, i.e., when the reaction was interrupted immediately upon reaching 80 °C, was called the "primary solution". In each case, the samples were placed in an ice bath upon reaching the desired hydrothermal treatment time.

The long-range order structure of the samples was investigated by X-ray diffraction (XRD) using a Rigaku D/Max-2500PC diffractometer, with Cu k_α ($\lambda = 1.5406$ Å) radiation. To undertake the XRD analysis, the sample was deposited on a glass substrate, which was placed on a heating plate at 50 °C to remove the solvent (water). The size and morphology of the vanadium oxide nanostructures were determined using, respectively, a Zeiss VP Supra 35 field emission scanning transmission electron microscope (FE-STEM) and a JEOL JEM 3010 URP high-resolution transmission electron microscope (HRTEM), operating at 300 KeV. FEG-STEM and HRTEM images were obtained from samples deposited in thin film form on a copper grid covered with a thin layer of carbon.

The mean width distribution of all the samples was estimated based on the measurement of at least 350 nanoribbons appearing in the FE-STEM images and by fitting the resulting distribution using a Gaussian function.

3. Results and discussion

Fig. 1 presents the XRD patterns of the samples obtained from the precursor solution, the primary solution (0 min of heat-treatment) and the solution subjected to 7200 min of treatment.

The XRD patterns of all the samples display a series of 00l diffraction peaks, confirming a preferential orientation in the c direction [26]. These diffraction peaks were indexed as $V_2O_5nH_2O$ monoclinic phase [26]. This behavior confirms that the hydrothermal treatment at this temperature did not cause any significant change in the long-range order structure of these samples, which is in good agreement with our previous results [26].

Fig. 2a and b present, respectively, the FE-STEM images of the precursor solution and the solution treated for 7200 min. Fig. 2a and b shows the presence of nanoparticles in nanoribbon form, which is consistent with the XRD results. An analysis of Fig. 2b reveals the presence of nanoribbon-to-nanoribbon attachment in the sample treated for 7200 min. This morphology and behavior, i.e., nanoribbon-to-nanoribbon attachment, was also observed in all the samples under study and therefore will not be presented here. This behavior indicates that the growth process related to an increase in the width of these $V_2O_5nH_2O$ nanoribbon samples can be described by the oriented attachment mechanism [22,23]. Liu et al. [22] observed a similar behavior in the hydrothermal treatment of ZnO nanorods, which also led to the formation of a "larger" ZnO crystal, i.e., the oriented attachment of the nanocrystals formed a "larger" ZnO crystal. Recently, Portehault et al. [23] also reported the growth of γ-MnO_2 nanocones through the oriented attachment of γ-MnOOH nanorods.

To study in greater detail the growth process of these nanoribbons, which, according to Fig. 2, occurs by the coarsening of two nanoribbons side by side, the kinetics of the coarsening process was investigated by measuring the width of nanoribbons in precursor solution hydrothermally heat-treated for different period of times. For illustration purposes, Figs. 3a and b show, respectively, the mean width distribution in the primary solution (0 min) and in the as-prepared solution treated for 7200 min.

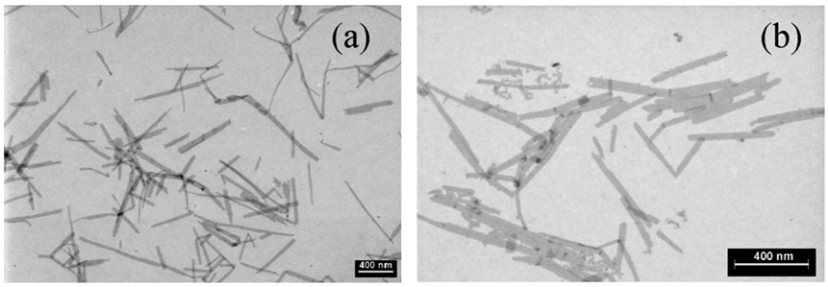

Fig. 2. FE-STEM images of precursor solution (a) and solution treated for 7200 min (b).

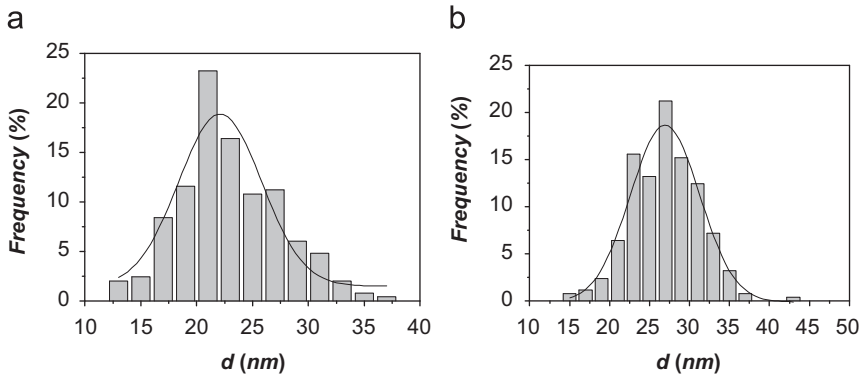

Fig. 3. (a) Mean width distribution of nanoribbons in the primary solution and (b) in the solution subjected to hydrothermal treatment for 7200 min.

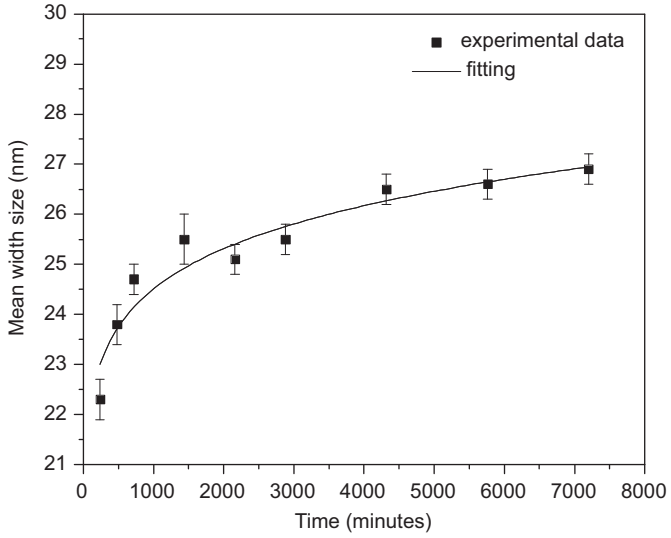

Fig. 4. Evolution of the nanoribbon's mean width as a function of hydrothermal treatment time.

Fig. 4 shows the mean width of nanoribbons as a function of hydrothermal treatment time. We can clearly observe the evolution from the primary solution from the significant growth of the nanoribbon width as a function of hydrothermal treatment time, as well as the fact that the width of the nanoribbons does not vary significantly from 4000 to 7200 min of hydrothermal treatment.

As can be seen in Fig. 4, the evolution of nanoribbon width displays a sharp increase for short periods of treatment up to 1000 min. As the treatment time increases, this variation is very low and tends to stabilize starting from 4000 min. This growth kinetics is very similar to that observed in other anisotropic materials subjected to hydrothermal treatment [17–20]. It is clear that the experimental behavior observed here cannot be fitted by the equation that describes the Ostwald ripening mechanism [16]. On the other hand, the classic equation used to describe the OA mechanism can also not be used, because this mechanism considers the process involving spherical particles where the term r_i^3 is derived from the particle volume [20]. In fact, the model denoted as the polymerization approach appears to be the most suitable one, since it was applied considering the active surface of the nanoparticles—in this case the nanoribbons' width [25]. Eq. (1), which describes the crystal growth kinetics in the polymerization OA model, was used to analyze the crystal growth kinetics of nanoribbon width. In this case, the term x_{max} in Eq. (1) is related to the nanoribbon width (w) of the nanostructures as a function of treatment time and the nanoribbon width of primary particles (w_0), i.e., $x_{max}=w/w_0$. The experimental data was fitted by this model, considering w_0 as a constant [25], with a nanoribbon width of 22.1 nm. The analysis of Fig. 4 indicates that the fitting of experimental data (line in Fig. 4) using the polymerization approach equation, Eq. (1), fits quite well. The fitting parameter, R^2, was found to be equal to 0.92, whereas the α value is equal to 0.041 ± 0.005. According to this model, a low value of α is expected because, as observed in the STEM images, the length of attached nanoribbons varies significantly, affecting the nanoribbon side coarsening process. Ribeiro et al. [25] reported a similar low value of α in the case of a higher dispersion of events. An important point in this kinetic model is related to primary solution (primary nanoribbons) considered as the sample obtained at "0" time of hydrothermal treatment. It is very difficult to affirm that no coalescence occurs in this condition, although the treatment time is equal to zero. Moreover, the proposed model is based on the hypothesis that each nanoparticle will coalesce only twice. From Fig. 2b one can see that more than two points of coalescence may occur.

Thus, although the experiments were limited to only one treatment temperature, the relatively good agreement of the OA

polymerization approach to the experimental data suggests that this mechanism is present in the evolution of width growth of the $V_2O_5nH_2O$ nanoribbons obtained under hydrothermal conditions.

The formation of defects, such as dislocations and/or twin boundaries at the nanoparticle interface, has also been observed in the coalescence process of nanostructured materials when the OA mechanism occurs [18,20]. Thus, it seems interesting to analyze in greater detail the interfacial region between two $V_2O_5nH_2O$ nanoribbons after coalescence. Unfortunately, we observed that the $V_2O_5nH_2O$ presenting nanoribbon morphology is highly unstable in the presence of the electron beam due to the large amount of intercalated water in its structure. This suggests that a more dehydrated form should be used in order to observe the defects that could be present at the interface between nanoparticles after coarsening. In a previous work, we showed that $V_2O_5 0.5H_2O$ with nanorod morphology containing a smaller amount of intercalated water can be obtained at 200 °C for 24 h [26]. We also observed that the difference in the amount of water, n, between these samples treated at 80 and 200 °C does not affect the growth direction in which we are interested. Therefore, the analysis applied to nanoribbons is also applicable to nanorods. In fact, Lee et al. [20] showed that an increase in the synthesis temperature plays an important role in increasing the degree of coalescence in the OA mechanism, which could be related to an increase in nanoparticle mobility and consequently of collision frequency. As a result, in our case, it is expected that raising the temperature causes the degree of coalescence to increase, similarly to what has been observed in other nanostructures.

Confirming this supposition, Fig. 5a and b shows the nanorod-to-nanorod attachment in the sample treated at 200 °C for 24 h. Fig. 5c shows a HRTEM image of attached nanorods. The regions identified as A and B correspond, respectively, to one nanorod and to the interface of two attached nanorods. From the analysis of an expanded HRTEM image of region A, Fig. 5d, one can see that the distance between neighboring planes is about $b=0.36$ nm along the nanorod's length and about $a=0.64$ nm along its width. These distances are related, respectively, to the (0 1 0) and (2 0 0) crystallographic planes in the $V_2O_5nH_2O$ nanostructure [26]. These features indicate that in the first step, growth occurs preferentially along the [0 1 0] direction (nanoparticle length), which, according to the literature, is attributed to the OR mechanism [27]. In the second step, growth occurs along the [1 0 0] direction (nanoparticle width), following the OA mechanism.

Region B in Fig. 5c was analyzed in more detail to verify the existence of defects in the region of coalescence. Fig. 5e shows the presence of dislocations in the region of coalescence, confirming that growth in the width (along the [1 0 0] direction) is governed by the OA mechanism.

In summary, the results reported here indicate that, under hydrothermal conditions, the OA mechanism appears to be an effective process in the growth of $V_2O_5nH_2O$ 1-D nanostructures.

4. Conclusion

The growth kinetics of $V_2O_5nH_2O$ nanoribbons was studied by subjecting a precursor solution to a hydrothermal treatment at 80 °C for different periods of time. The evolution of the nanoribbons' width in this hydrothermal condition indicated that oriented attachment (OA) plays an important role in the growth mechanism of these samples. The variation in nanoribbon width as a function of treatment time was well fitted by the OA polymerization approach, and the presence of defects in the region of nanoparticle coalescence confirmed the OA mechanism in the [1 0 0] direction. These results therefore show that the OA mechanism occurs as a second growth step, and that the first one is the OR mechanism in the [0 1 0] direction, i.e., the nanoparticle length. In summary, the results reported in this work provide a better understanding of the growth kinetics of $V_2O_5nH_2O$ 1-D nanostructures in hydrothermal conditions, allowing for better control of the growth or shape of 1-D anisotropic nanostructures.

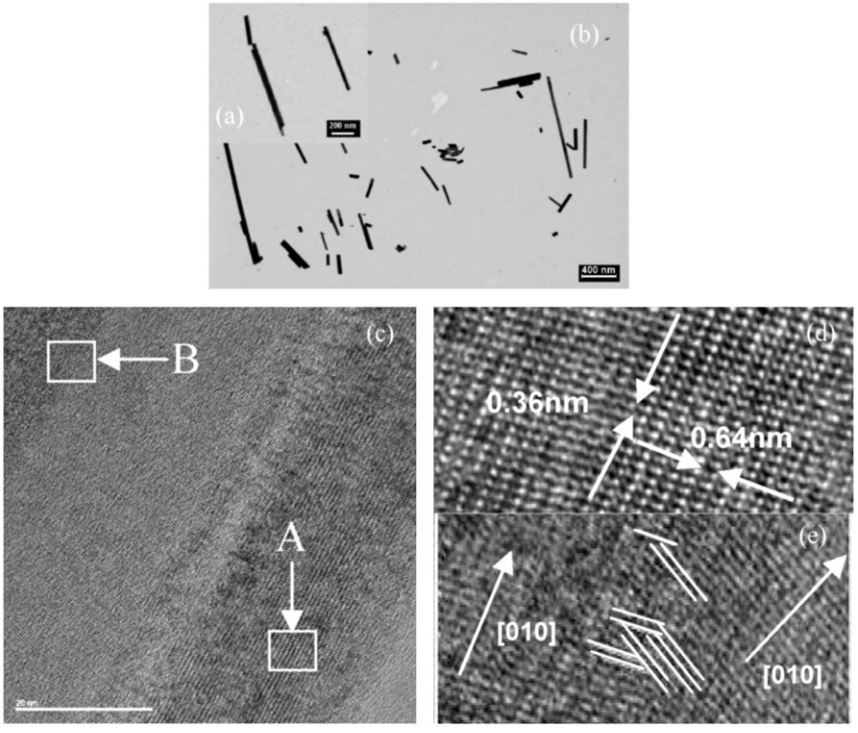

Fig. 5. (a) and (b) FE-STEM image of nanorods; (c) HRTEM images showing the side attachment of nanorods and an expanded HRTEM image of region A (d) and region B (e).

Acknowledgements

The authors gratefully acknowledge the financial support of the Brazilian research funding agencies FAPESP and CNPq, and thank the Electron Microscopy Laboratory (LME) of the Brazilian National Synchrotron Light Laboratory (LNLS) for the use of its HRTEM microscopy facility.

References

[1] C. Karunakaran, S.J. Senthilvelan, Colloid Interface Sci. 289 (2005) 466.
[2] B. Li, Y. Xu, G. Rong, M. Jing, L. Xie, Nanotechnology 17 (2006) 2560.
[3] J. Liu, X. Wang, Q. Peng, Y. Li, Adv. Mater. 17 (2005) 764.
[4] H. Serier, M.-F. Achard, O. Babot, N. Steunou, J. Maquet, J. Livage, C. Leroy, R. Backov, Adv. Funct. Mater. 16 (2006) 1745.
[5] C.M. Leroy, M.F. Achard, O. Babot, N. Steunou, P. Masse, J. Livage, L. Binet, N. Brun, R. Backov, Chem. Mater. 19 (2007) 3988.
[6] C. Imawan, H. Steffes, F. Solzbacher, F. Obermeier, Sens. Actuators B 77 (2001) 346.
[7] C.R. Xiong, A.E. Aliev, B. Gnade, K.J. Balkus, ACS NANO 2 (2008) 293.
[8] Y. Wang, G. Cao, Chem. Mater. 18 (2006) 2787.
[9] N. Pinna, U. Wild, J. Urban, R. Schlogl, Adv. Mater. 15 (2003) 329.
[10] E.A. Ponzio, T.M. Benedetti, R.M. Torresi, Electrochim. Acta 52 (2007) 4419.
[11] V. Petkov, P.N. Trikalitis, E.S. Bozin, J.L. Billinge, T. Vogt, G. Kanatzidis, J. Am. Chem. Soc. 124 (2002) 10157.
[12] S. Gao, Y. Chen, H. Luo, L. Jiang, B. Ye, M. Wei, K.J. Wei, J. Nanosci. Nanotechnol. 8 (2008) 3500.
[13] D. Pan, Z. Shuyuan, Y. Chen, J.G. Hou, J. Mater. Res. 17 (2002) 1981.
[14] F. Zhou, X. Zhao, C. Yuan, L. Li, Cryst. Growth Des. 8 (2008) 723.
[15] G. Li, L. Jiang, H. Peng, Mater. Lett. 61 (2007) 4070.
[16] J.M. Lifshitz, S.S. Slyozov, J. Phys. Chem. Solids 119 (1961) 35.
[17] C. Ribeiro, H.E.J. Lee, T.R. Giraldi, J.A. Varella, E. Longo, E.R. Leite, J. Phys. Chem. B 108 (2004) 15612.
[18] E.J.H. Lee, C. Ribeiro, E. Longo, E.R. Leite, J. Phys. Chem. B 109 (2005) 20842.
[19] E.R. Leite, C. Vila, J. Bettini, E. Longo, J. Phys. Chem. B 110 (2006) 18088.
[20] E.J.H. Lee, C. Ribeiro, E. Longo, E.R. Leite, Chem. Phys. 328 (2006) 229.
[21] M. Niederberger, H. Golfen, Phys. Chem. Chem. Phys. 8 (2006) 3271.
[22] B. Liu, H.C. Zeng, J. Am. Chem. Soc. 125 (2003) 4430.
[23] D. Portehault, S. Cassaignon, E. Baudrin, J.P. Jolivet, Cryst. Growth Des. 6 (2009) 2562.
[24] Y. Wang, J. Zhang, Y. Yang, F. Huang, J. Zheng, D. Chen, F. Yan, Z. Lin, C. Wang, J. Phys. Chem. B 111 (2007) 5290.
[25] C. Ribeiro, E.J.H. Lee, E. Longo, E.R. Leite, Chem. Phys. Chem. 7 (2006) 664.
[26] W. Avansi, C. Ribeiro, E.R. Leite, V.R. Mastelaro, Cryst. Growth Des. 9 (2009) 3626.
[27] F. Zhou, X. Zhao, C. Yuan, L. Li, Cryst. Growth Des. 8 (2008) 723.